J. Membrane Biol. 99, 103–111 (1987)

The Journal of
Membrane Biology

An Anion Channel of Sarcoplasmic Reticulum Incorporated into Planar Lipid Bilayers: Single-Channel Behavior and Conductance Properties

Manabu Tanifuji,* Masahiro Sokabe,† and Michiki Kasai

Department of Biophysical Engineering, Faculty of Engineering Science, Osaka University, Toyonaka, Osaka 560, Japan, and †Department of Physiology, Nagoya University School of Medicine, Nagoya 466, Japan

Summary. An anion channel of sarcoplasmic reticulum vesicle has been incorporated into planar lipid bilayers by means of a fusion method and its basic properties were investigated. Analysis of fusion processes suggested that one SR vesicle contained approximately one anion channel. The conductance of this channel has several substates and shows a flickering behavior. The occupation probability of each substate was voltage dependent, which induced an inward rectification of macroscopic currents. Further, the anion channel was found to have the following properties. (1) The single-channel conductance is about 200 pS at 100 mM Cl^-. (2) The channel does not select among monovalent anions but SO_4^{2-} hardly permeates through the channel. (3) SO_4^{2-} added to the *cis* side (the side to which SR vesicles were added) inhibits Cl^- current competitively in a voltage-dependent manner. (4) An analysis of this voltage dependence suggests that the binding site of SO_4^{2-} is located at about 36% of the way across the channel from the *cis* entrance.

Key Words sarcoplasmic reticulum · lipid bilayer · anion channel · single channel · substate · channel blockade

Introduction

Ca^{2+} release and uptake of sarcoplasmic reticulum (SR) have been studied by many researchers for understanding the mechanism of excitation contraction coupling (reviewed by Martonosi, 1984). Associated with these investigations it has been shown that SR membrane is permeable for monovalent cations and anions (Kasai & Miyamoto, 1976; Meissner & McKinley, 1976). Although physiological role of these pathways for monovalent ions is not clear, there is a possibility that they make some contributions to Ca^{2+} release and/or uptake mechanisms. From this point of view it is necessary to characterize each of them. Permeability of SR membrane was initially studied by the tracer method (Kasai & Miyamoto, 1976; Meissner & McKinley, 1976; Kasai, 1981). However, various important ions such as Na^+, K^+ and Cl^- permeate so fast that their time courses could not be followed. Although the turbidity method applied to SR vesicles enabled us to measure fast permeation processes comparable with that of water (Kometani & Kasai, 1978), the data suggested the existence of faster permeation processes of cations and anions which could not be followed by these methods (Kasai et al., 1985).

Miller and Racker (1976) made it possible to measure the current through channels in SR vesicles by an incorporation of them into planar bilayers. This method allows us to measure faster permeation processes and to observe single-channel behaviors in SR vesicles. Miller (1978) found that the K^+ and Cl^- conductances increased with the incorporation of SR vesicles into planar bilayers, and that K^+ current fluctuated between conducting and nonconducting states which was regarded as open and closed states of a single channel. He and his co-workers have studied the properties of K^+ channel in detail (Coronado, Rosenberg & Miller, 1980; Labarca, Coronado & Miller, 1980; Coronado & Miller, 1982). On the other hand, little is known concerning the Cl^- current induced by SR vesicles. In this paper, to characterize the Cl^- channel of SR, we have studied the Cl^- current in detail. We made clear the single-channel behavior and basic channel properties, such as voltage dependence, ionic selectivity, and conductance-concentration relationship. We also found that SO_4^{2-} having low conductance blocked the channel in an asymmetric and a voltage-dependent manner. Although the physiological function of the channel is not known at present, our results should contribute to understanding its role in SR membranes.

Materials and Methods

Biochemicals

SR vesicles were prepared from rabbit white dorsal and leg muscle by the method of Miller and Rosenberg (1979) with slight modification. Muscle was homogenized in 0.18 M sucrose, 5 mM

* *Present address:* National Institute for Physical Sciences, Myodaiji, Okazaki 444, Japan.

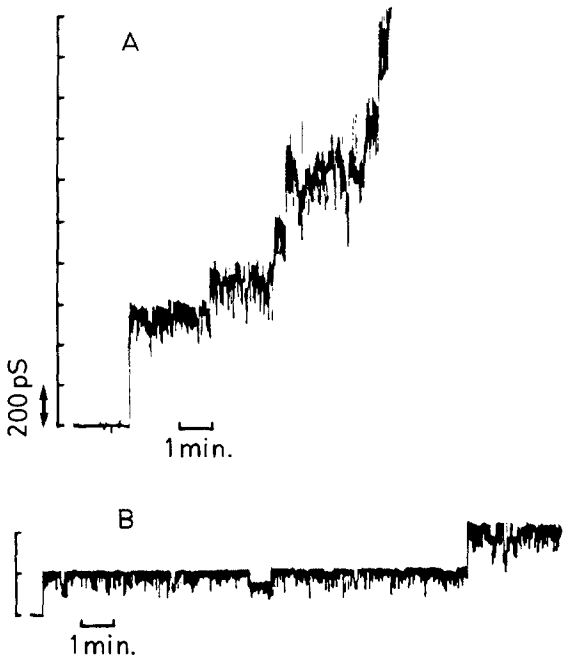

Fig. 1. Time course of conductance increase of planar bilayers after addition of SR vesicles. Both sides of the membrane contained 100 mM cholineCl, 5 mM HEPES-Tris, pH 7.2, and holding potential was −50 mV. (*A*) Cl^- conductance increase in staircase fashion. The rising phase of each step reflected fusion of a single vesicle. In this case five or six vesicles fused with a planar bilayer sequentially. (*B*) Single-channel conductance fluctuation observed after the first vesicle fused. In each trace the ordinate was graduated for the unit of conductance (200 pS)

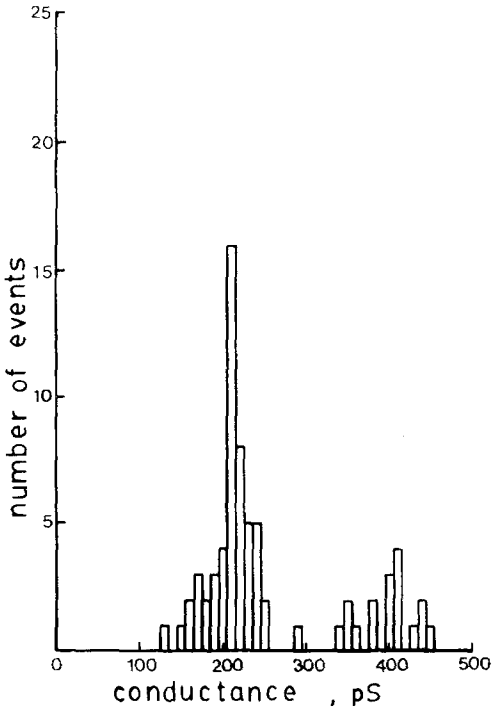

Fig. 2. Histogram of conductance height of fusion steps. Conductance increases caused by SR vesicle fusion were measured as in Fig. 1 for 70 fusion events

HEPES-KOH, pH 7.5. The homogenates were adjusted to pH 7.0 with KOH, and were centrifuged at 900 × *g* for 7 min. The supernatant was centrifuged at 9,000 × *g* for 12 min and its supernatant was centrifuged at 53,000 × *g* for 60 min. The pellet was suspended in 0.4 M sucrose, 5 mM HEPES-KOH, pH 7.5, and the suspension was centrifuged at 5,000 × *g* for 10 min. The supernatant was then centrifuged at 53,000 × *g* for 60 to 90 min and the pellet was suspended in 0.4 M sucrose, 5 mM HEPES-KOH, pH 7.5, to a protein concentration of 25 to 50 mg/ml. This preparation was stored in small aliquots at −70°C.

Asolectin (Type II-S) used for artificial planar bilayers was purchased from Sigma Chemical Co., USA. This Asolectin already contained some amounts of anionic lipids which were necessary for the SR vesicle fusion with bilayers. Other reagents were commercial products of analytical grade. $CholineClO_4$, $choline_2SO_4$, and $Tris_2SO_4$ were prepared by neutralization of base solutions with acid solutions.

Electrical

Planar bilayers were formed by the method of Mueller and Rudin (1969). Asolectin solution (14.7 mg/ml in *n*-decane) was applied to a hole (about 500 μm in diameter) on a polypropylene or polystyrene partition which divided a polyvinylchloride trough into two aqueous chambers. Each chamber was filled with about 4 ml of buffer solutions. Detail of the system was almost the same as Miller's (Miller & Rosenberg, 1979). The solutions used were composed of $choline^+$, Li^+, or $Tris^+$ salt of various anions buffered with 5 mM HEPES-Tris, pH 7.2. These solutions were chosen to avoid the contamination of cation conductance (Coronado et al., 1980; Coronado & Miller, 1982).

Each chamber was connected to an Ag/AgCl electrode via a glass salt bridge, and the electrical conductance of planar bilayers was measured by a current-to-voltage converter under voltage-clamp conditions. Experiments were carried out at room temperature, 25 ± 2°C.

Fusion of SR Vesicles

Fusion of SR vesicles with planar bilayers occurred under appropriate conditions, i.e., anionic lipid in the artificial membrane, Ca^{2+} in aqueous medium, and an osmotic gradient across SR membranes (Miller & Racker, 1976). After thinning of the membrane, $CaCl_2$ (1 to 4 mM final concentration) and SR vesicles (10 to 50 μg/ml final concentration) were added with stirring to one side of the membrane. Within a few minutes the membrane conductance began to increase in discrete steps which reflected fusion of SR vesicles with the planar bilayer. Allowing enough time to pass, fusion would stop as the dissipation of osmotic gradient across SR vesicles, and the membrane conductance reached a constant value defined as the "macroscopic level." Single-channel currents were measured by controlling the amount of Ca^{2+} and/or SR vesicles added so as to decrease fusion events. The *cis* side of the membrane was defined as the side to which SR vesicles were added; and the *trans* side was defined as the opposite side. The voltage across the membrane was defined with respect to the *trans* side.

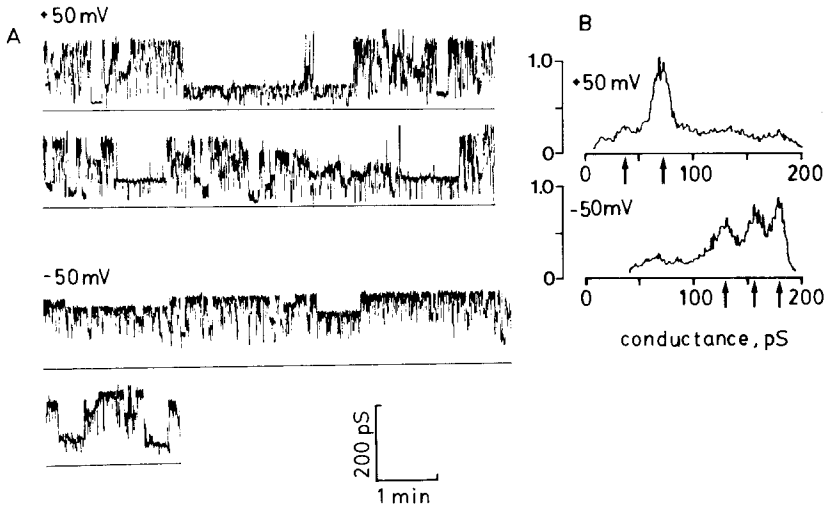

Fig. 3. Single-channel current traces at different voltages. (*A*) Current fluctuations recorded at the holding potential of either +50 or −50 mV, with a symmetrical solution containing 100 mM cholineCl, 5 mM HEPES-Tris, pH 7.2. The solid line in each trace represents the zero-current level, and the channel opening is upward deflection. (*B*) Amplitude histograms obtained from the traces. Conductance is shown at the abscissa and the height represented the occupation frequency of each conductance level in arbitrary units. At least five peaks shown by arrows could be discriminated in this case, and their occurrence at two voltages were different

Results

Insertion of Anion Channels

Figure 1(*A*) shows a typical conductance increase caused by SR vesicle fusion with a planar bilayer in 100 mM cholineCl buffer. Since K^+ channels of SR vesicles do not carry choline$^+$ (Coronado & Miller, 1982), the conductance increase should be the result of SR vesicles fused with a planar bilayer containing Cl^- channels. In fact, as shown later, a reversal potential measurement confirmed that the current was carried by Cl^-. The conductance increased in discrete steps, each of which seems to correspond to the fusion of a single vesicle. Since each step did not show the same size, individual vesicles seem to contain different numbers of Cl^- channels. The step size in Fig. 1(*A*) suggests that there exists a unit size conductance, 200 pS. Figure 2 shows a histogram of conductance height up to 500 pS. The distribution of conductance step has two well-defined peaks. One peak has the amplitude of about 200 pS, and the other had twofold amplitude, 400 pS. In the case of conductance steps higher than 500 pS, the size had amplitudes of integral multiples of 200 pS, while peaks having amplitudes between the multiples or lower than 200 pS were hardly observed. From these results, we can conclude that the unit step size corresponds to the single-channel conductance of the Cl^- channel, about 200 pS at 100 mM Cl^-.

The mean number of channels in a single vesicle can be estimated from the analysis of fusion processes. The histogram of conductance height of fusion steps shows that the peaks are seen at 200 and 400 pS (Fig. 2). The events which fell in the range of 100 to 300 pS and those in the range of 300 to 500 pS were counted as the vesicles containing one channel and those containing two channels, respectively. Assuming the Poisson distribution of the number of channels in each vesicle, we obtained 0.69 for the mean number of channels in a single vesicle.

On decreasing the amount of Ca^{2+} and/or SR vesicles applied, the conductance fluctuations following a single vesicle fusion could be observed, as shown in Fig. 1(*B*). Some conductance levels and rapid disruption of conductance were observed. The fluctuation which has a maximum conductance of 200 pS was regarded as a single-channel current fluctuation (fluctuation of the single channel itself). The single-channel current fluctuations showed voltage dependence as shown in Fig. 3(*A*). Figure 3(*B*) shows the histogram of the current fluctuations. The current fluctuation has two well-defined features: (1) existence of several states which have different conductance levels, and (2) rapid disruption of current. At least four sublevels can be discriminated between open and closed states in this case. Unfortunately, since the number and amplitude of sublevels were variable from membrane to membrane, we could not determine the precise nature of the substates. The reasons why the distribution of conductances in Fig. 2 did not fit to a summation of two Gaussian distributions and the peaks shown in Fig. 2 were not so sharp may be attributable to the existence of sublevels.

Voltage Dependence

As shown in Fig. 4, the maximum current through the single channel is a linear function of potentials, but macroscopic current becomes sublinear in a positive potential region. Figure 3 shows that the maximum current is almost the same at −50 and +50 mV, but that the occupation frequency of each

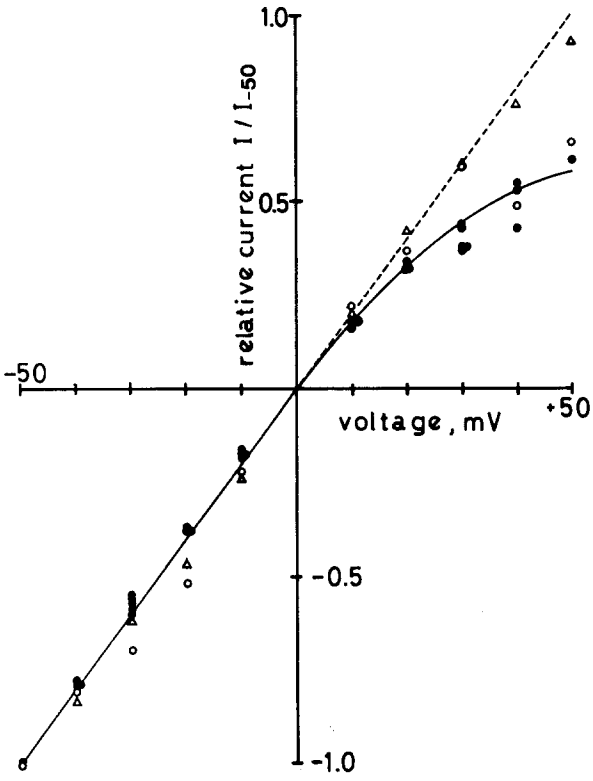

Fig. 4. Current-voltage relationships for single-channel currents and for macroscopic currents. Both sides of membrane contained 100 mM cholineCl, 5 mM HEPES-Tris, pH 7.2. Relative current indicates I/I_{-50} where I is the current at the holding potential and I_{-50} is that at −50 mV. Macroscopic currents (●). Maximum current (△) and time-average current (○) obtained from single-channel recordings

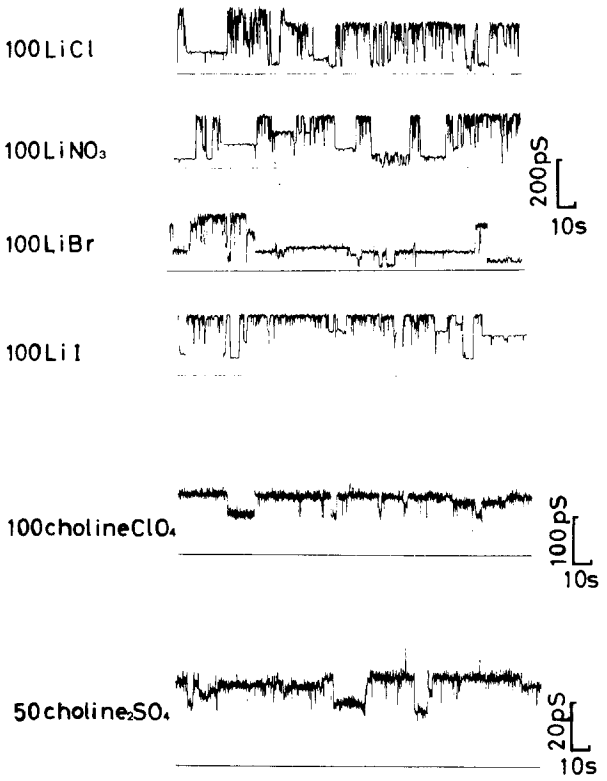

Fig. 5. Single-channel conductance fluctuations in various anions. Channel fluctuations were recorded with symmetrical solution containing anions indicated by each trace (in millimolar concentration). The solid line in each trace indicates the zero-current level. Holding potential was +50 mV for all traces

substate is quite different at −50 and +50 mV. The occupation frequency of relatively large substates at −50 mV decreases at +50 mV. This implies that the voltage dependence of macroscopic current is originated from the voltage dependence of occupation probability of sublevels in the single channel. Actually, the time-averaged current through the single channel at respective potentials well predicts the voltage dependence of the macroscopic current (Fig. 4).

Ion Selectivity

Selectivity for anion over cation was estimated with reversal potential measurement under asymmetric concentration of LiCl. Using 300 and 100 mM LiCl in a *cis* and a *trans* chamber, the single-channel currents were reversed at +20 mV. From this value the permeability ratio of Li^+ to Cl^- was estimated by the Nernst equation to be 0.15. Selectivity among anions were estimated from conductance ratios and permeability ratios obtained from single-channel conductance and reversal potential under bi-ionic conditions. Figure 5 shows fluctuations of single-channel conductance in symmetrical solutions of 100 mM Cl^-, NO_3^-, Br^-, I^-, ClO_4^-, and 50 mM SO_4^{2-}. Two common features of the current fluctuations, sublevels and flickering behavior, can be seen, while the amplitude of single-channel conductances is different among those anions. Although the single-channel conductance for Cl^- was estimated only from fusion steps in Fig. 1, here the single-channel conductance will be estimated more precisely. The conductance of planar bilayer itself was estimated from the lowest current level at +50 mV where the channel could be regarded as being at the completely closed state. The difference of conductances between maximum and minimum levels was employed as the single-channel conductance. The single-channel conductance for Cl^- was calculated to be 198 pS (100 mM Cl^-), which was consistent with the value obtained from the fusion steps in Fig. 1.

Permeability ratios for various anions versus Cl^- were obtained from reversal potentials accord-

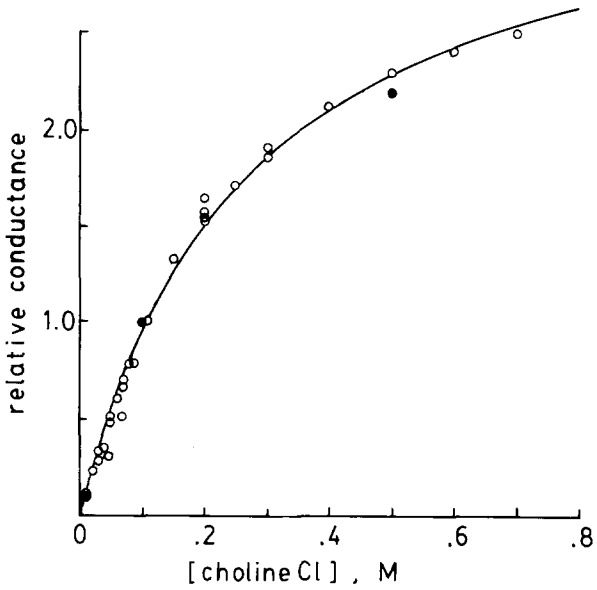

Fig. 6. Conductance-concentration relationship. Conductances obtained from the single channel (●) and macroscopic (○) measurements were normalized with the values at 100 mM cholineCl. Single-channel conductances were obtained from the fusion height in symmetrical solutions indicated on the abscissa. Macroscopic conductances were measured by adding the appropriate amount of cholineCl to both sides of the membrane. All sets of points were obtained from a single membrane. Each solution also contained 5 mM HEPES-Tris, pH 7.2 and 1 to 4 mM $CaCl_2$ on the *cis* side. Holding potential was −50 mV. The curve was drawn according to Eq. (1), where K_1 = 265 mM and g_{max} is 3.50-fold of the conductance at 100 mM Cl^-. These values were determined by the method of least squares for the data above 50 mM Cl^-

ing to the Goldman equation. The reversal potentials, at which the direction of the currents reversed, were obtained from macroscopic and microscopic measurements under bi-ionic conditions. In the Table, single-channel conductances, their ratio versus the single-channel conductance of Cl^-, and the permeability ratios are summarized. Both single-channel conductance ratio and permeability ratio of monovalent anions were almost the same. It is also shown that monovalent anions are almost equally permeable, but SO_4^{2-} is quite less permeable.

Conductance-Concentration Relationship

Figure 6 shows the conductance-concentration relationships of Cl^- conductance. Conductances were measured at symmetric Cl^- concentrations except that the *cis* solution contained 1 to 4 mM $CaCl_2$. At Cl^- concentrations lower than 50 mM, $CaCl_2$ in the *cis* side should have some contribution on the conductances, and the conductances might be overestimated at the holding potential of −50 mV where Cl^- flows from the *cis* side to the *trans*. At concentrations above 50 mM Cl^- the data could be fitted with a simple saturation curve,

$$g = \frac{g_{max}}{1 + \frac{K_1}{[Cl^-]}} \quad (1)$$

where K_1 is the dissociation constant for Cl^-, and g_{max} is the maximum conductance (Fig. 6). Their values obtained by curve fitting were: K_1 = 265 mM and g_{max} is 3.50-fold of the conductance at 100 mM Cl^-.

Table. Selectivity of SR anion channel[a]

Ion(X^-)	γ_X (pS)	γ_X/γ_{Cl}	P_X/P_{Cl}
Cl^-	198	1.0	1.0
NO_3^-	208	1.1	1.3
Br^-	209	1.1	1.2
I^-	179	0.9	—
ClO_4^-	140	0.7	1.2
SO_4^{2-}	15	0.08	0.04

[a] Single-channel conductances γ_X were determined from differences between maximum and minimum conductance levels as in Fig. 4. The ratios of single-channel conductances γ_X/γ_{Cl} were calculated from the average values of single-channel conductances. Reversal potentials were measured at asymmetric ionic compositions, that is, 100 mM X^- (or 90 mM X^- and 10 mM Cl^-) on one side of the membrane and 100 mM Cl^- (90 mM Cl^- and 10 mM X^-) on the other side. Exceptionally in the case of SO_4^{2-}, 50 mM SO_4^{2-} on one side of the membrane and 100 mM Cl^- on the other side were used. The permeability ratios, P_X/P_{Cl}, were calculated from reversal potentials according to the Goldman equation. In all experiments, Li^+, $Tris^+$ and/or $choline^+$ were used as counter-ions of salt solutions. The mean values obtained from at least two membranes are shown here except the single-channel conductance of NO_3^-, I^-, and SO_4^{2-}, which were obtained from single membranes.

SO_4^{2-} Inhibition

Since the permeability for SO_4^{2-} is quite low, as seen in the Table, it was expected that SO_4^{2-} could inhibit the Cl^- current. As shown in the inset of Fig. 7, when SO_4^{2-} was added to the *cis* side at the holding potential of −50 mV, the single-channel current of Cl^- was actually inhibited. The effect of SO_4^{2-} was immediate and reversible (*data not shown*). On the contrary, no inhibition was observed when SO_4^{2-} was added to the *trans* side at the holding potential of either −50 or +50 mV.

Figure 7 shows the inhibition of conductance by SO_4^{2-} at several Cl^- concentrations. The inhibition depended on the Cl^- concentration. Higher concentrations of SO_4^{2-} were required to get the same extent of inhibition at higher concentrations of Cl^-. To analyze these data, a competitive inhibition model

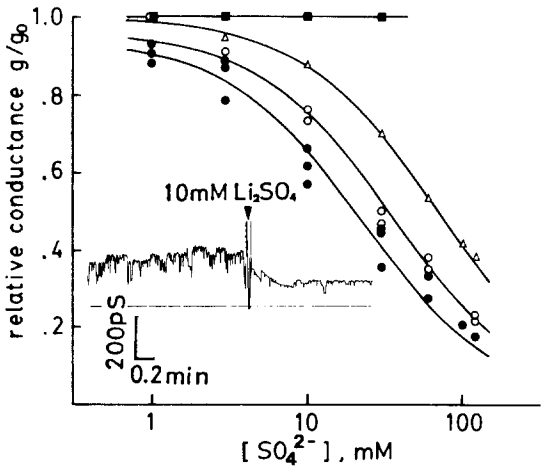

Fig. 7. Inhibition of Cl^- current by SO_4^{2-}. Relative Cl^- conductances, normalized with the value obtained without SO_4^{2-}, were plotted against SO_4^{2-} concentrations. The aqueous solutions contained 100 mM (●, ■), 200 mM (○), and 500 mM (△) of cholineCl and 5 mM HEPES-Tris, pH 7.2 in both sides of the membrane. Either Li_2SO_4 or $choline_2SO_4$ was added to the *trans* side (■) or the *cis* side (●, ○, △). Significant difference could not be found whether cholineCl or LiCl were used. Holding potential was −50 mV for the addition of SO_4^{2-} to the *cis* side and +50 mV for that to the *trans* side. Furthermore, no effect was also observed at −50 mV for the addition to the *trans* side. The continuous curves were drawn according to Eq. (2) using the value of K_{app} obtained from Fig. 8. The trace of single channel shows the effect of 10 mM Li_2SO_4 added to the *cis* solution. A horizontal line in the trace represents zero-current level. It can be seen that conductance levels of substate with SO_4^{2-} are lower than those without SO_4^{2-}. This implies that SO_4^{2-} inhibits the conductance of sublevels as well as the maximum conductance, and our precise analysis shows their rates of inhibition are equal (*data not shown*)

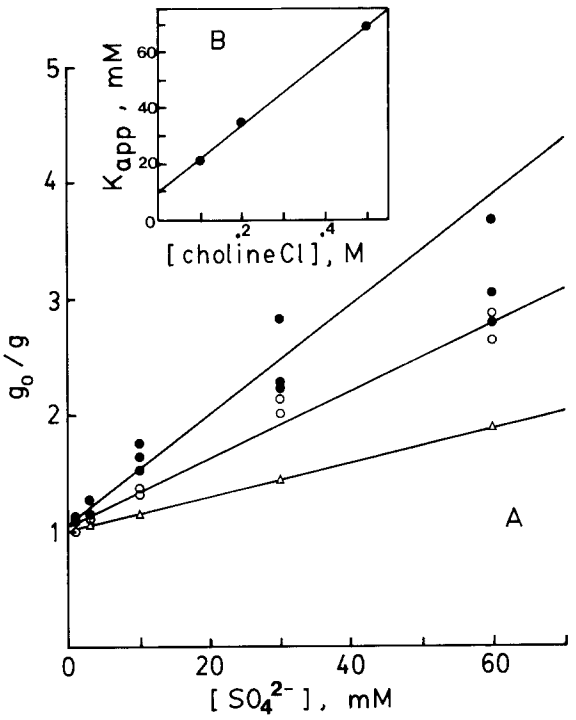

Fig. 8. Reciprocal plots of relative conductances versus SO_4^{2-} concentration. (*A*) The reciprocal of relative conductances, g/g_0, obtained in Fig. 7 were plotted against SO_4^{2-} concentrations. Cl^- concentrations were 100 mM (●), 200 mM (○), and 500 mM (△). Solid lines were drawn according to Eq. (2). The slope, the reciprocal of K_{app}, of each line was determined by the method of least squares for all data except the case of 100 mM Cl^-. The slope for 100 mM Cl^- was calculated from the data below 30 mM SO_4^{2-}. (*B*) The K_{app} obtained from (*A*) were plotted against Cl^- concentrations. The solid line was drawn according to Eq. (3). The intercept and the slope of the line were determined by the method of least squares and the dissociation constant for Cl^- $K_1 = 87.2$ mM, and the dissociation constant for SO_4^{2-} $K_2 = 10.2$ mM, were obtained

by SO_4^{2-} was considered. Neglecting the contribution of SO_4^{2-} current, the conductance in the presence of SO_4^{2-} is given by

$$g = \frac{g_0}{1 + \dfrac{[SO_4^{2-}]}{K_{app}}} \tag{2}$$

where g_0 is the conductance without SO_4^{2-}, and K_{app} is the apparent dissociation constant for SO_4^{2-}. When the reciprocals of the conductances are plotted against the SO_4^{2-} concentrations, linear relations were obtained except for the data at 100 mM Cl^- (Fig. 8*A*). In the case of 100 mM Cl^- the data were not fitted with a straight line. Probably the SO_4^{2-} current was not small enough to neglect compared with the Cl^- current at such low Cl^- concentrations. If we assume that Cl^- conductance saturates according to Eq. (1) and the competition between SO_4^{2-} and Cl^- occurs at the Cl^- binding site, K_{app} is given by

$$K_{app} = K_2\left(1 + \frac{[Cl^-]}{K_1}\right) \tag{3}$$

where K_1 is the dissociation constant for Cl^- and K_2 is the dissociation constant for SO_4^{2-}. The values of K_{app} were obtained from the slopes in Fig. 8(*A*) and were plotted as a function of Cl^- concentrations in Fig. 8(*B*). The data were fitted with a straight line and K_1 and K_2 are obtained to be 87.2 and 10.2 mM, respectively. If the noncompetitive inhibition occurred, the slope should be constant for any concentrations of Cl^-. Thus the result precludes such a possibility.

Another aspect of the SO_4^{2-} inhibition was its voltage dependence. The inhibition by SO_4^{2-} at negative voltage was recovered when the voltage was turned to positive value (Fig. 9 inset). As shown in

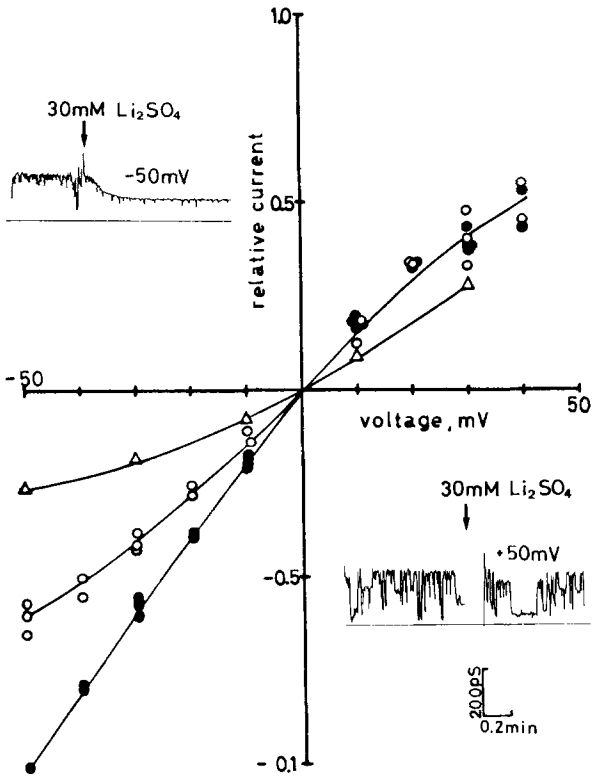

Fig. 9. Voltage dependence of SO_4^{2-} blockade. Macroscopic currents were plotted against voltages. $Choline_2SO_4$ was added to the *cis* side. Both sides of the membrane contained 100 mM cholineCl, 5 mM HEPES-Tris, pH 7.2. Currents were normalized with the current at −50 mV before adding $choline_2SO_4$. The continuous curves were drawn by eye. Concentrations of $choline_2SO_4$ were 0 mM (●), 10 mM (○), and 60 mM (△). Single-channel recordings of SO_4^{2-} blockade at −50 and +50 mV are shown in the inset. Additions of 30 mM Li_2SO_4 to the *cis* side were shown by arrows. Horizontal lines in the trace represent zero-current level. Holding potentials are given in the trace

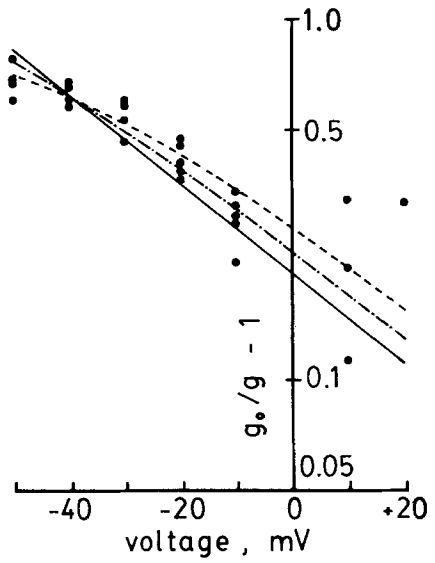

Fig. 10. Linearized plot of voltage dependence of SO_4^{2-} blockade. Macroscopic conductance was measured at various voltages when 10 mM $choline_2SO_4$ was added to the *cis* side. Both sides of the membrane contained 100 mM cholineCl, 5 mM HEPES-Tris, pH 7.2, $g_0/g - 1$ was plotted against the voltage according to Eq. (5), where g_0 and g were the conductance before and after the addition of SO_4^{2-}. The solid line was drawn according to Eq. (5) using $K_{app}(0) = 53$ mM and $\delta = 0.36$, which were obtained by the method of least squares for the data. The other two curves were drawn according to Eq. (6), assuming that the values for $k_2(0)/k_1(0)$, $K_{app}(0)$ and δ are 0.1, 34 mM and 0.36 (----) and 0.04, 42 mM and 0.36 (-·-·-·-), respectively

Fig. 9, the inhibition of macroscopic current was dependent on the applied voltage when a small amount of SO_4^{2-} was added to the *cis* side. At negative voltages SO_4^{2-} blocked strongly the Cl^- current, but at positive voltages SO_4^{2-} was less effective on the Cl^- current. Although there is no unique interpretation for this behavior, the simplest one assumes that a blocking ion moves part of the way across the membrane to form a blocking complex. In such a condition, the electrical field acting on the charged ligand would contribute to the standard free energy of the binding reaction. Thus, $K_{app}(V)$, the dissociation constant for the SO_4^{2-} binding reaction, should vary exponentially with the voltage according to

$$K_{app}(V) = K_{app}(0) \exp\left(-\frac{z\delta FV}{RT}\right) \quad (4)$$

where $K_{app}(0)$ is the apparent dissociation constant at zero voltage, δ is the fraction of the total electrical potential drop across the membrane found at the SO_4^{2-} binding site, z is the valency of the blocking ion (in this case $z = -2$), and F, R, and T have the usual meaning. Combining Eq. (2) and Eq. (4), we obtain

$$\ln\left(\frac{g_0}{g} - 1\right) = \ln\left(\frac{[SO_4^{2-}]}{K_{app}(0)}\right) + \frac{z\delta FV}{RT}. \quad (5)$$

According to this equation a plot of $\ln(g_0/g - 1)$ *vs.* voltage should give a straight line. As shown in Fig. 10, the data were fitted with a straight line in the range from −50 to +10 mV, and we could obtain $\delta = 0.36$ and $K_{app}(0) = 53$ mM. Thus, assuming a constant intramembrane electrical field, we suggest that the site of SO_4^{2-} binding is about 36% of the way across the channel from the *cis* entrance.

The experimental data, however, show slightly low values from the straight line at −50 mV. Probably these deviations might arise from the penetration of SO_4 ions to the *trans* side at negative voltages. In such a case, the following scheme can be postulated.

$$SO_4^{2-}{}_{cis} \underset{k_{-1}}{\overset{k_1}{\rightleftharpoons}} X \cdot SO_4^{2-} \xrightarrow{k_2} SO_4^{2-}{}_{trans}$$

where X represents the site for SO_4^{2-}. From this scheme we could obtain the following equation (Woodhull, 1973):

$$\frac{g_0}{g} - 1 = \frac{[SO_4^{2-}]}{K_{app}(0) \exp\left(-\frac{z\delta FV}{RT}\right)\left\{1 + \frac{k_2(0)}{k_1(0)} \exp\left(\frac{zFV}{RT}\right)\right\}}. \quad (6)$$

Assuming that the values of $k_2(0)/k_1(0)$, $K_{app}(0)$ and δ are 0.1, 34 mM and 0.36 (for the upper dotted curve) and 0.04, 42 mM and 0.36 (for the lower dotted curve), respectively, a better fit than the straight line could be obtained as shown in Fig. 10.

Discussion

It has been shown that SR membranes are highly permeable for Cl^- as well as K^+ (Kometani & Kasai, 1978). However, it is difficult to measure such Cl^- permeation processes directly by the conventional photometric methods. In this paper we could study the Cl^- permeation process at the single-channel level by using the bilayer technique. It has become apparent that the SR membrane contains an anion channel with a large conductance and weak selectivity; the single-channel conductance is about 200 pS in 100 mM Cl^-.

Substates and Flickering Event

Single-channel recordings showed that the current fluctuation of the anion channel has two characteristics: existence of four or five substates and flickering behavior. It is possible that these sublevels reflect the number of different or same kind of channels incorporated into the planar bilayer at one time. If so, we could observe current fluctuations corresponding to each of such channels. But this was not the case for the anion channel of SR. Recently, several reports have shown the existence of anion channels having substates and flickering behavior (Gray, Bevan & Ritchie, 1984; Nelson, Tang & Palmer, 1984; Krouse, Schneider & Gage, 1986). These studies also pointed out the large single-channel conductance and weak selectivity of the channels. There seemed to be a class of large conductance and weak selectivity anion channels having substates and flickering events.

Voltage Dependence at Macroscopic and Single-Channel Level

Voltage dependence of the SR anion channel was inconsistent with that studied by Miller in his early work with bilayers (1978). He described the voltage independence of macroscopic Cl^- conductance. On the contrary, we found that the increase of macroscopic Cl^- current was less than that expected from linearity at positive potentials. This result was confirmed by the observation of voltage-dependent occupation frequency of substates of single anion channels. The most frequently observed sublevels were different at -50 and $+50$ mV, and the time-averaged single-channel currents were consistent with the macroscopic current-voltage relationship (Figs. 3 and 4). Thus it is concluded that the channel has obvious voltage-dependent property.

Effect of SO_4^{2-} on the Anion Channel

We found that SO_4^{2-} hardly permeated through the channel in contrast to monovalent anions, and that *cis* SO_4^{2-} inhibited Cl^- current (Fig. 7). Since *trans* SO_4^{2-} did not affect the Cl^- conductance, effects of ionic strength difference and a surface potential change produced by the addition of SO_4^{2-} were neglected. Precise study of SO_4^{2-} inhibition of Cl^- current shown in Fig. 8 led us to the conclusion that SO_4^{2-} blocks the channel with a single-site competitive blocking model; SO_4^{2-} enters the channel from the *cis* side, binds to the Cl^- binding site, prevents the binding of Cl^- to the site, and consequently blocks the movement of Cl^- through the channel as long as it occupies the site. The fact that no blockade was observed from the *trans* side indicates asymmetric configuration of the channel. Furthermore the analysis of voltage-dependent blockade shows that the site exists at 36% of the way across the channel from the *cis* entrance (Fig. 10).

In the above discussion, SO_4^{2-} current was neglected because of its low permeability. But actually SO_4^{2-} could permeate through the channel a little and its current caused the deviations from the straight lines both in Fig. 8 and Fig. 10. The analysis of SO_4^{2-} blockade, as well as the saturation experiment, revealed the single occupancy for Cl^-, but the dissociation constant for Cl^- was approximately three times smaller than that obtained from the saturation experiment (Fig. 6 and Fig. 8). One possible reason for this discrepancy may arise from the surface potential produced by anionic lipid in planar bilayers. In a low salt concentration range surface potential of bilayers should lower the salt concentration at membrane-solution interface. In the case

of SO_4^- blockade, as the experiments were done at relatively high Cl^- concentration (≧ 100 mM), such effect should not be significant. However, the shape of the curve in the saturation experiment at 0 to 50 mM Cl^- concentration produces significant change of the dissociation constant. As a result the value obtained from the saturation experiment might be overestimated.

Density of the Channel in SR Vesicles

To suggest the functional role of the anion channel, it is important to know the density of the channels and their distribution in SR membrane. The mean number of the anion channel in a single vesicle was estimated to be 0.69 from the analysis of fusion steps by assuming the Poisson distribution and the equal probability of fusion. It has been estimated that a single vesicle contains about four hundred pump proteins (Martonosi, 1984) and at least ten K^+ channels (Labarca et al., 1980). These numbers of ion channels are consistent with the observation in the reconstitution experiments (1.4 anion channels and 19 cation channels per vesicle, Morimoto and Kasai, 1986). Further, a fluorescence quenching experiment also suggested the small number of anion channels per vesicle (Nunogaki & Kasai, 1984). Recently, we observed similar Cl^- channels in the heavy fraction of SR vesicles. Thus the Cl^- channel, as well as the pump proteins, is probably the common channel in the SR membrane.

This work was supported by a Grant-in-Aid for Special Project Research on Mechanism of Bioelectrical Response (61107003) from the Japanese Ministry of Education, Science and Culture.

References

Coronado, R., Miller, C. 1982. Conduction and block by organic cations in a K^+-selective channel from sarcoplasmic reticulum incorporated into planar phospholipid bilayers. *J. Gen. Physiol.* **79**:529–547

Coronado, R., Rosenberg, R.L., Miller, C. 1980. Ionic selectivity, saturation, and block in a K^+-selective channel from sarcoplasmic reticulum. *J. Gen. Physiol.* **76**:425–446

Gray, P.T.A., Bevan, S., Ritchie, J.M. 1984. High conductance anion-selective channels in rat cultured Schwann cells. *Proc. R. Soc. London B* **221**:395–409

Kasai, M. 1981. Inhibition of the anion permeability of sarcoplasmic reticulum vesicles by some stilbene derivatives. *J. Biochem.* **89**:943–953

Kasai, M., Miyamoto, H. 1976. Depolarization-induced calcium release from sarcoplasmic reticulum fragments II. Release of calcium incorporated without ATP. *J. Biochem. (Tokyo)* **79**:1067–1076

Kasai, M., Nunogaki, K., Nagasaki, K., Tanifuji, M., Sokabe, M. 1985. Ion channels of sarcoplasmic reticulum vesicles and calcium release. *In:* Structure and Function of Sarcoplasmic Reticulum. S. Fleischer and Y. Tonomura, editors. pp. 537–560. Academic, New York

Kometani, T., Kasai, M. 1978. Ionic permeability of sarcoplasmic reticulum vesicles measured by light scattering method. *J. Membrane Biol.* **41**:295–308

Krouse, M.E., Schneider, G.T., Gage, P.W. 1986. A large anion-selective channel has seven conductance levels. *Nature (London)* **319**:58–60

Labarca, P., Coronado, R., Miller, C. 1980. Thermodynamic and kinetic studies of the gating behavior of a K^+-selective channel from the sarcoplasmic reticulum membrane. *J. Gen. Physiol.* **76**:397–424

Martonosi, A.N. 1984. Mechanisms of Ca^{2+} release from sarcoplasmic reticulum of skeletal muscle. *Physiol. Rev.* **64**:1240–1320

Meissner, G., McKinley, D. 1976. Permeability of sarcoplasmic reticulum membrane. The effect of charged ionic environments on Ca^{2+} release. *J. Membrane Biol.* **30**:79–98

Miller, C. 1978. Voltage-gated cation conductance channel from fragmented sarcoplasmic reticulum: Steady-state electrical properties. *J. Membrane Biol.* **40**:1–23

Miller, C., Racker, E. 1976. Ca^{++}-induced fusion of fragmented sarcoplasmic reticulum with artificial planar bilayers. *J. Membrane Biol.* **30**:283–300

Miller, C., Rosenberg, R.L. 1979. A voltage-gated cation conductance channel from fragmented sarcoplasmic reticulum. Effects of transition metal ions. *Biochemistry* **18**:1138–1145

Morimoto, T., Kasai, M. 1986. Reconstitution of sarcoplasmic reticulum Ca^{2+}-ATPase vesicles lacking ion channels and demonstration of electrogenicity of Ca^{2+}-pump. *J. Biochem. (Tokyo)* **99**:1071–1080

Mueller, P., Rudin, D.O. 1969. Biomolecular lipid membranes. Techniques of formation, study of electrical properties, and induction of ionic gating phenomena. *In:* Laboratory Techniques in Membrane Biophysics. H. Passow and R. Stampfli, editors. pp. 141–156. Springer-Verlag, Berlin

Nelson, D.J., Tang, J.M., Palmer, L.G. 1984. Single-channel recordings of apical membrane chloride conductance in A6 epithelial cells. *J. Membrane Biol.* **80**:81–89

Nunogaki, K., Kasai, M. 1984. Ion permeation through sarcoplasmic reticulum membrane. *In:* Transmembrane Signaling and Sensation. F. Oosawa, T. Yoshioka and H. Hayashi, editors. pp. 217–227. Japan Scientific Societies Press, Tokyo

Woodhull, A.M. 1973. Ionic blockage of sodium channels in nerve. *J. Gen. Physiol.* **61**:687–708

Received 19 February 1987; revised 24 June 1987